The preparation and reactivity of metal-containing monomers 54.* Thermolysis of the acrylamide monomer $[Co(CH_2{=}CHCONH_2)_4(H_2O)_2](NO_3)_2$

A. S. Rozenberg, A. V. Raevskii, E. I. Aleksandrova, O. I. Kolesova, G. I. Dzhardimalieva, and A. D. Pomogailo

Institute of Problems of Chemical Physics, Russian Academy of Sciences, 142432 Chernogolovka, Moscow Region, Russian Federation. Fax: +7 (096) 515 3588. E-mail: adpomog@icp.ac.ru

The kinetics and pathways of thermolysis of the Co(II) complex with acrylamide, $[Co(CH_2{=}CHCONH_2)_4(H_2O)_2](NO_3)_2$ (**1**) were studied. The rate of gas evolution is satisfactorily approximated by a first-order equation of autocatalysis. The composition of gaseous and solid products of thermolysis of **1** was studied by IR spectroscopy, mass spectrometry, and electronic microscopy. Thermal transformations of acrylamide complex **1** include three macro stages: dehydration, polymerization of the dehydrated monomer, and thermooxidative destruction of the resulting polymer.

Key words: acrylamide complexes of cobalt nitrate, thermal transformations, dehydration, solid-phase polymerization, thermooxidative destruction, cobalt nano-sized particles.

The complexes of acrylamide (AAm) with transition metal nitrates are of interest as regards the possibility of thermally initiated frontal polymerization (FP) and the manufacture of metal-containing materials (including nano-sized materials) by high-temperature pyrolysis. Previously,[2] the AAm complexes $[M(CH_2{=}CHCONH_2)_4](NO_3)_n \cdot xH_2O$, where M = Cr^{III}, Mn^{II}, Fe^{III}, Co^{II}, Ni^{II}, Cu^{II}, and Zn^{II}; n = 2, 3; x = 0, 2, were synthesized and characterized by X-ray diffraction analysis, and the phenomenology[3] and characteristic features[4] of frontal polymerization of complexes with Mn^{II}, Co^{II}, Ni^{II}, and Zn^{II} nitrates were studied. Polymerization of these metal-containing monomers takes place in the temperature range of 353—373 K; the addition of radical inhibitors retards this process.

In order to extend the views on the transformation pathways of AAm complexes both in the frontal polymerization and in the pyrolysis, in this work, we studied the kinetic features and possible pathways of thermal transformation in relation to the monomer $[Co(CH_2{=}CHCONH_2)_4(H_2O)_2](NO_3)_2$ (**1**), which was characterized by X-ray diffraction analysis.[2]

Experimental

The acrylamide complex **1** was synthesized by previously published procedures.[5,6] Found (%): C, 29.6; H, 5.0; Co, 11.5. $C_{12}H_{24}CoN_6O_{12}$. Calculated (%): C, 28.6; H, 4.8; Co, 11.7. The powder consists of shapeless agglomerates (blocks) of particles with sizes of <10 μm (ρ = 1.53 g cm^{-3}), colored pink in the reflected light.

Thermolysis of complex **1** was studied under nonisothermal conditions in air (C derivatograph (MOM, Hungary)) in the temperature range of 273—873 K (heating rate 10 K min^{-1}). The kinetics of isothermal transformation was studied based on gas evolution in a static nonisothermic reactor at the temperature T_{therm} = 463—553 K. The heated volume with the studied compound was ~0.05 V, where V is the reactor volume. The size of the cylindrical tube was maintained constant (internal diameter $d_{in} \approx 4$ mm), weighed portion $70 \cdot 10^{-3}$ g (in some cases, thermolysis was carried out in tubes with $d_{in} \approx 6$ mm). The transformation kinetics was monitored using a diaphragm null pressure gage. The thermal decomposition of monomer **1**, including that during the FP, was carried out in a self-generated atmosphere. The sample was preliminarily evacuated at ~20 °C and ~1 Pa for 30 min. In the case of FP, ignition of the samples (powder of **1** pressed to form a 30—50 mm-long cylinders ~4 mm in diameter) was performed at the ignition temperature T_{ig} = 438 K.

The total amount of gaseous products evolved at ~20 °C, the amount of these products in the low-temperature (77 K) fractionation and, the loss of mass by the sample (Δm, g) were measured. The gaseous and condensed products of transformation of compound **1** were studied by IR spectroscopy in the 400—4000 cm^{-1} region (a Specord IR-75 spectrophotometer). In addition, the gaseous products were analyzed by mass spectrometry using an MS-3701 quadrupole mass spectrometer (EI, 75 eV). The solid products of transformation of complex **1** were examined by optical microscopy (OM) on the hot stage of an MBI-6 instrument. The electron-microscopy studies were performed using an HU-125 transmission electron microscope with an accelerating voltage of 100 kV. The powder X-ray diffraction patterns were obtained on a DRON UM-2 diffractometer using Cu-Kα-radiation.

The magnetic properties of powders were studied qualitatively using reactions of the solid products on exposure to a constant magnetic field.

Results and Discussion

Characteristic features of heat evolution in the thermolysis of complex 1. The results of thermoanalytical

* For Part 53, see Ref. 1.

Published in Russian in *Izvestiya Akademii Nauk. Seriya Khimicheskaya,* No. 5, pp. 862—867, May, 2001.

1066-5285/01/5005-901 $25.00

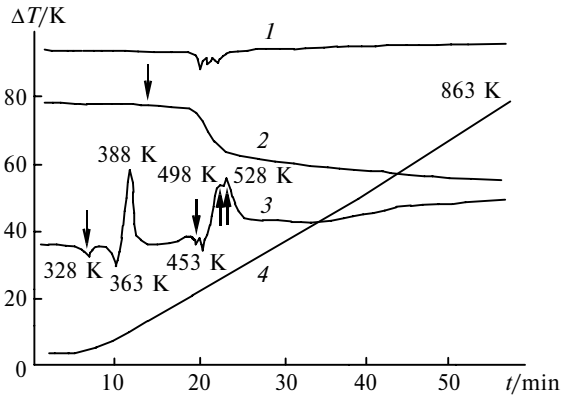

Fig. 1. Derivatogram of complex **1**: (*1*) DTGA ($dm/dt \cdot 0.8$/g min^{-1} mm^{-1}); (*2*) TGA ($\Delta m \cdot 2.5 \cdot 10^3$/g mm^{-1}); (*3*) DTA ($\Delta T \cdot 0.88$/K min^{-1} mm^{-1}); (*4*) TA ($T \cdot 0.5$/K mm^{-1}). Heating rate 10 K min^{-1}, sample mass $45.8 \cdot 10^{-3}$ g.

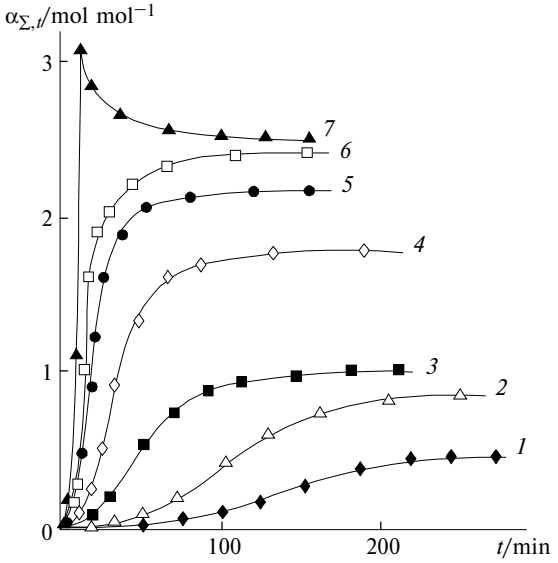

Fig. 2. Kinetics of gas evolution in the thermolysis of complex **1** under different temperature conditions (K): (*1*) 463 (0.46); (*2*) 468 (0.81); (*3*) 473 (0.98); (*4*) 483 (1.78); (*5*) 493 (2.22); (*6*) 503 (2.40); (*7*) 503 (~2.48). The $\alpha_{\Sigma,t}$ values are given in parentheses. Curves *1*—*5*, *7*: d_{in} = 4 mm, *6*: d_{in} = 6 mm.

studies point to a complex pattern of transformations of compound **1** (Fig. 1). The thermograms exhibit the following thermal effects: a weak endotherm at 328—333 K; a weak endotherm at 358—363 K passing into a strong exotherm with a maximum at $T_{max} \approx 388$ K; a poorly resolved region of thermal effects at 453—495 K; and a complex exotherm (strong) in the region of 498—578 K with $T_{max} \approx 528$ K. The major mass loss (Δm >50% (w/w)) takes place at 453—578 K. In the region of endothermic effects and the exothermic peak at 388 K, Δm < 10% (w/w). The endothermic effect (359—363 K) related to the formation of the liquid phase (melting) is immediately followed by heat evolution (364 K) caused by polymerization of monomer **1**.

Kinetics of gas evolution in the thermolysis of complex 1 under isothermal conditions. When thermolysis is carried out in the self-generated atmosphere at T_{therm} = 463—553 K and the dimensions of the initial sample are constant ($d_{in} \approx 4$ mm, $m_0 = 70 \cdot 10^{-3}$ g), the kinetics of evolution of gaseous products at different temperatures corresponds to two transformation modes $\alpha_\Sigma(t) = \alpha_{\Sigma,t}$, where $\alpha_{\Sigma,t}$ is the number of gas moles evolved by the instant t per mole of the initial substance (Fig. 2). For T_{therm} < 493 K, at short transformation times (corresponding approximately to the time of sample warming-up ($t_0 \approx$ 4—5 min)), a step of gas evolution takes place, $\alpha_{\Sigma,t} = \alpha_{\Sigma,0} \approx 0.3$; after that, the dependence $\alpha_{\Sigma,\tau} = \alpha_{\Sigma,t} - \alpha_{\Sigma,0}$, where $\tau = t - t_0$, shows an S-shaped pattern (see Fig. 2, curve *1*—*6*). Up to the degree of gas evolution $\eta \le 0.9$, the rate of the process W is approximated satisfactorily by a first-order equation of autocatalysis

$$W = d\eta/dt = k(1 - \eta)(\eta + \xi_0),$$

where $k = 4.2 \cdot 10^7 \exp[-24000/(RT)]$ s^{-1}; $\xi_0 \approx 1.9 \cdot 10^{-2}$; $\eta = (\alpha_{\Sigma,t} - \alpha_{\Sigma,0})/(\alpha_{\Sigma,f} - \alpha_{\Sigma,0})$; $\alpha_{\Sigma,f}$ is gas evolution over the whole transformation time. The difference $\alpha_{\Sigma,f} - \alpha_{\Sigma,0}$ depends on the process temperature and increases as the temperature rises:

T_{therm}/K	463	468	473	483	493
$\alpha_{\Sigma,f} - \alpha_{\Sigma,0}$/mol mol^{-1}	0.46	0.81	0.98	1.78	2.22

When $T_{therm} \ge 503$ K and the dimensions of the sample remain constant, the curve of gas evolution in the thermolysis of complex **1** passes through an extremum (see Fig. 1, curve *7*). Raising the temperature (T_{therm} = 503—553 K) shifts the gas evolution maximum $\alpha_{\Sigma,max}$ toward shorter times of transformation. When the sample size changes ($d_{in} \approx 6$ mm), the gas evolution is again described by a smooth S-shaped curve $\alpha_{\Sigma,\tau}$ (see Fig. 2, curve *6*). This peculiar "explosive" behavior of the temperature dependence of $\alpha_{\Sigma,\tau}$ is, apparently, caused by the pattern of heat and mass transfer during thermal destruction and might be one of the reasons for the propagation of FP.

Evolution of the topography of solid products. According to optical microscopy data, the initial complex **1** powder consists of dispersed particles looking as shapeless blocks colored pink (in the reflected light). The consistent temperature OM scanning of the samples in air revealed a complex pattern of transformations. In the 273—333 K temperature range, the situation does not change. At 333—358 K (the region of endothermic effects in the thermograms), the liquid phase containing monodisperse solid particles is evolved. The pink coloring of the liquid can, apparently, be explained by dissolution of the initial material. An increase in the temperature to 361—385 K results in the formation of a virtually continuous solid, colorless, optically active (in crossed polarization filters) material with a minor admixture of the liquid phase. At 385 K, the optical

activity vanishes. No structural analysis of compound **1** was carried out in this transformation region. However, the available data concerning solid-phase processes imply that the loss of optical activity by a solid can be due either to chemical transformations (this is unlikely under the given conditions) or to the transition of the sample to an isotropic modification (for example, cubic).

The phase transition is followed ($T > 385$ K) by one more formation of the liquid phase and dissolution of the solid. This process is accompanied by gas evolution and ends by 399 K. On further increase in the temperature to 413 K, the relatively thick pink-colored melt is transformed into a viscous shrunken matrix. At temperatures of >453 K, vigorous gas evolution from this viscous matrix takes place; this gives rise to a new optically active solid phase. The material transparency disappears at 483 K.

The topographic features of the products formed at different degrees of thermal transformation of powdered **1** in the self-generated atmosphere as well as the products of transformations of prelimiarily pressed powders during the FP indicate that the morphological pattern observed is similar to the evolution of the topography of powdered **1** during pyrolysis in air.

For comparison, we performed an OM study of the thermal decomposition of AAm in air; the samples used were dispersed powders consisting of colorless well-faceted optically active (in crossed polarization filters) crystals with a small number of defects. It was found that in the temperature range of 349—361 K, melting ($T_{пл}$ = 357.5 K)[8] and simultaneous sublimation of AAm take place. The non-melted substance, which is, apparently, the product of polymerization, does not exhibit optical activity. Further raising the temperature does not change qualitatively the topography of the solid-phase products. The monodisperse colorless inclusions found in the liquid phase upon thermolysis of complex **1** (333—358 K) might be due to partial evolution of AAm upon dissociation of complex **1**.

The composition of the gaseous products of thermolysis. The overall amount of gaseous products evolved upon thermolysis in the self-generated atmosphere at the end of decomposition of complex **1** increases with an increase in T_{therm} (Table 1). As $\alpha_{\Sigma,f}$ increases, the mass loss becomes more pronounced. However, the found values for the mass loss are markedly lower than the values expected for the thermooxidative destructive polymerization of complex **1**, for example, at the maximum possible degree of conversion by the reaction

$$[Co(CH_2{=}CHCONH_2)_4(H_2O)_2](NO_3)_2 =$$
$$= CoO_x + (1/n)(8 - y)(—CH_2—)_n + 4\ CO + 3\ N_2O +$$
$$+ 0.5(4 - x - 3y)O_2 + (4 + y)H_2O,$$

where $\alpha_{\Sigma,f} \geq 7.0$ at $\Delta m_f \leq 58.5\%$ (w/w).

According to the results of analysis of the IR absorption spectra, the major gaseous products of the thermolysis of complex **1** are CO, N_2O, and CO_2. In addition, traces of NH_3 and H_2O vapor are formed. No C—H-containing products were detected in the gas phase.

Table 1. Gas evolution ($\alpha_{\Sigma,f}$) and the loss of mass by the sample (Δm_f) upon the thermolysis of complex **1** in the self-generated atmosphere

T_{therm}/K	$\alpha_{\Sigma,f}$/mol mol^{-1}	Δm_f (% (w/w))
463	0.76	20.6
468	1.08	23.0
473	1.29	24.0
483	2.10	31.0
503	2.70	38.0

More comprehensive information about the composition of the gaseous products of thermolysis of **1** was derived from mass spectrometry. The data of IR absorption spectra are consistent in kind with the results provided by mass spectrometry; however, the latter implies a much more intricate composition of the gaseous products. The most intense peaks in the mass spectra* are $m/z = 28^+$ (100), in which the major contribution can come from $[N_2]^+$ (100), $[CO]^+$ (100), $[C_2H_4]^+$ (100), and $[C_2H_6]^+$ (100); $m/z = 30$ (10—50) — $[NO]^+$ (100), $[NO_2]^+$ (100), $[CH_3NO_2]^+$ (100); $m/z = 44$ (30—60) — $[CO_2]^+$ (100), $[N_2O]^+$ (100), $[CH_2CHC(O)NH_2]^+$ (89.2). Analysis of the mass spectra shows that the gaseous products of transformation comprise mainly CO, N_2, CO_2, N_2O, and NO. Calculations showed that the relative yields of these substances at the final stage vary as functions of T_{therm} and amount to (% v/v): CO (30—38), N_2 (20—25), CO_2 (16—20), N_2O (10—15), and NO (0—10). As the T_{therm} increases, the contents of N_2O, NO, and CO in the product mixture decrease, while those of N_2 and CO_2 increase. According to mass spectrometry, the qualitative composition of the gas phase formed in the FP in the self-generated atmosphere is generally close to the composition of thermolysis products formed at 463—553 K, namely, CO, N_2, CO_2, N_2O, H_2O, and NH_3, the greatest contribution to the gas evolution being made by CO, CO_2, and N_2O. However, the gas evolution level $\alpha_{\Sigma,f}$ at the end of FP is 0.1—0.2 (for Δm_f = 2—4% (w/w)), which is much lower than that in the case of thermolysis.

The ratio of the yields of gaseous products varies during the thermolysis at a constant temperature. The evolution of mass spectra during the "explosive" decomposition of complex **1** is most illustrative (Fig. 3). When $\alpha_{\Sigma,t}$ reaches the maximum, the greatest contribution to gas evolution is made by NO (see Fig. 3, curve *6*); after the maximum has been passed ($\alpha_{NO,max} \approx 1.4$), the amount of NO drops almost to zero with simultaneous decrease in $\alpha_{\Sigma,t}$. Unlike the $\alpha_{NO,t}$ curve, which passes through an extremum, the yields $\alpha_{CO_2,t}$ and $\alpha_{N_2,t}$ increase slightly and monotonically after the $\alpha_{\Sigma,t}$ function

* From here on, the values in parentheses are I_{rel} (%) of peaks in the mass spectrum (at different T_{therm}) and peaks of individual compounds.

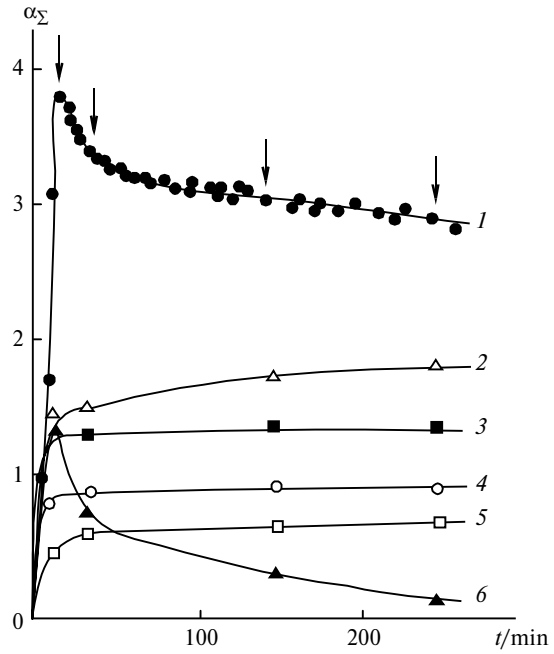

Fig. 3. Yield of gaseous products of transformation of complex **1** during the "explosive" decomposition at 513 K: (*1*) $\alpha_{\Sigma,t}$; (*2*) $3\alpha_{CO_2,t}$; (*3*) $3\alpha_{N_2O,t}$; (*4*) $\alpha_{CO,t}$; (*5*) $\alpha_{N_2,t}$; (*6*) $\alpha_{NO,t}$. The arrows mark the instant of sampling.

has reached the maximum, and $\alpha_{CO,t}$ and $\alpha_{N_2O,t}$ virtually do not change.* It is significant that, after the $\alpha_{\Sigma,t}$ value has reached the maximum ($\alpha_{\Sigma,max} \approx 3.71$ at $\Delta m_{max} = 42.7\%$ (v/v), see Fig. 3), the loss of mass by the sample decreases in parallel with gas evolution (to $\Delta m_f = 36.6\%$ (v/v) for $\alpha_{\Sigma,f} \approx 3.0$).

In other words, the processes occurring during further thermolysis after the $\alpha_{\Sigma,t}$ maximum has been reached, lead to a higher yield of the condensed phase. Among other reasons, this can be due to the consumption of NO (the intermediate product formed upon decomposition of complex **1**) for the formation of products condensed under the thermolysis conditions, in addition to other pathways of NO conversion, including the formation of N_2. The attenuation of the loss of mass by the sample with the extremal pattern of the gas evolution curve might be also due to the partial destruction of **1**, resulting in the liberation and evaporation of the AAm ligand followed by its condensation. This is indicated indirectly by the data on sublimation of free AAm on cold parts of the reactor during early stages of gas evolution (intense IR absorption bands of the sublimate in the region of stretching (ν), deformation (δ), and twisting (τ) vibrations, 3180—3350 ν(N—H), 1680 ν(C=O), 1615 ν(C=C), 1435 $\delta(CH_2)$, 1360 ν(C—N), and $\tau(NH_2)$ at 965, 990 cm^{-1}, typical of AAm).

One can suggest that the intermediate formation and consumption of NO during thermolysis of **1** also takes place in the case of "smooth" gas evolution but its yield is low, both during the process and at the end of decomposition due to the high rate of transformation of NO into N_2O and N_2.

Solid-phase products of thermolysis. The IR spectrum of complex **1** contains the following absorption bands (cm^{-1})*: 3360—3380 (s) $\nu(H_2O)$, 3190 (s) $\nu_s(N—H)$, 3290 (s) $\nu_{as}(N—H)$, 2800 (w) ν(C—H), 1665 (vs) ν(C=O), 1630 (m) ν(C=C), 1580 (m) δ(N—H), 1445 (m) $\delta(CH_2)$, 1385 (vs) $\nu_d(NO_3)$, 1355 (vs) ν(C—N), 1288 (m) δ(C—H), 1055 (m) $\nu_s(NO_3)$, 831 (m) $\pi(NO_3)$, 650 (ms) $\delta(NO_3)$. Comparison of the IR absorption spectra of the solid products of transformation of **1** formed during decomposition with the IR absorption spectrum of the initial sample revealed the following features. Even at low degrees of decomposition attained during warming-up of the sample, the IR absorption spectrum changes in kind. The $\nu(H_2O)$ absorption bands of complex **1** disappear. The absorption bands associated with the stretching vibrations of the AAm ligand are converted into two broad bands with maxima at 3360 and 1600 cm^{-1}. As this transformation takes place, the $\nu(CH_2)$ and $\delta(CH_2)$ bands are broadened and shift to lower frequencies, and the ν(C=C) band disappears. These data point to polymerization of the AAm ligand, which is confirmed by comparison of the changes in the IR spectra of AAm and the spectra of polyacrylamide.

In parallel with the increase in the degree of transformation, the intensity of the absorption bands corresponding to the NO_3^- anion in the spectra of the thermolysis products decreases (down to disappearance), indicating its decomposition.

According to powder X-ray diffraction data, the solid products formed during the process and at the end of gas evolution are X-ray amorphous.

Study of the topography of the final product of thermolysis of complex **1** by electron microscopy (Fig. 4) demonstrated that this product is a single-phase material consisting of shapeless glassy particles with a uniform electron density.

Pathways of thermolysis of complex 1. The results obtained point to a complex multichannel mechanism of **1** thermolysis.

According to X-ray diffraction data,[2] the crystals of **1** consist of octahedral $[Co(CH_2=CHCONH_2)_4(H_2O)_2]^{2+}$ cations and NO_3^- anions. The Co^{II} atom is coordinated through the O atoms of four AAm ligands and two H_2O molecules and the structural framework is formed by a three-dimensional system of hydrogen bonds between the NH_2 and NO_3 groups and between the coordinated H_2O molecules and the NO_3^- anions. In the initial complex cation of **1**, the Co—O distances are substantially dissimilar and range from 0.2965 to 0.2114 nm,

* The $\alpha_{i,t}$ values were calculated with the assumption that $\alpha_{\Sigma,t} \approx \alpha_{CO,t} + \alpha_{N_2,t} + \alpha_{CO_2,t} + \alpha_{N_2O,t} + \alpha_{NO,t}$.

* The designations in parentheses are the relative intensities of IR absorption bands of degenerate (d), symmetric (s) and asymmetric (as) stretching, deformation, and scissoring (δ) vibrations: vs is very strong, s is strong, ms is the medium-strong, m is medium, w is weak.

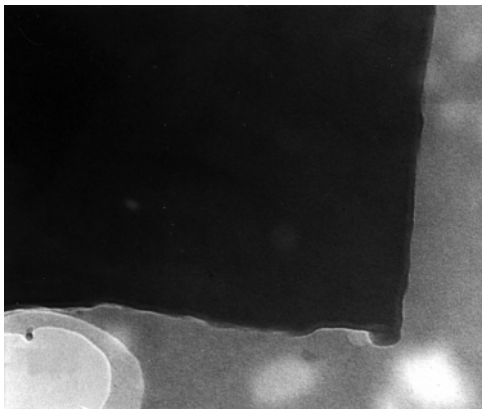

Fig. 4. Photomicrograph of the product of thermolysis of complex **1** at 523 K obtained by electron microscopy (magnification 100 000).

which points to nonequivalence of ligands and to energetic differences between the Co—O bonds. An increase in the temperature facilitates cleavage of the weakest Co—O bonds and promotes changes in the coordination environment of the cation.

At relatively low temperatures (328—362 K, the region of endothermic effects in the thermogram, see Fig. 1), dehydration of the crystal hydrate takes place even at low stages of transformation*

$$[Co(CH_2{=}CHCONH_2)_4(H_2O)_2](NO_3)_2\ (s.) \rightarrow$$
$$\rightarrow [Co(CH_2{=}CHCONH_2)_4](NO_3)_2\ (s.) +$$
$$+ 2\ H_2O\ (liq.) - 19\ kJ\ mol^{-1}. \qquad (1)$$

In addition, decomposition of the complex cation with partial elimination of the AAm ligand may also occur, for example, as follows:

$$[Co(CH_2{=}CHCONH_2)_4](NO_3)_2\ (s.) \rightarrow$$
$$\rightarrow [Co(CH_2{=}CHCONH_2)_2](NO_3)_2\ (s.) +$$
$$+ 2\ CH_2CHCONH_2\ (liq.) - 134.6\ kJ\ mol^{-1}. \qquad (2)$$

* The $\Delta H_f^\circ[Co(CH_2{=}CHCONH_2)_4(H_2O)_2(NO_3)_2\ (s.)] = -2362$ kJ mol^{-1}, $\Delta H_f^\circ[Co(CH_2{=}CHCONH_2)_4(NO_3)_2\ (s.)] = -1768$ kJ mol^{-1} and $\Delta H_f^\circ[Co(CH_2{=}CHCONH_2)_2(NO_3)_2\ (s.)] = -1096$ kJ mol^{-1} values were calculated on the basis of thermochemical estimates, by comparison of the heats of formation[7,8] in the series $CoCl_2\ (s.) \rightarrow CoCl_2 \cdot NH_3\ (s.) \rightarrow CoCl_2 \cdot 2NH_3\ (s.) \rightarrow CoCl_2 \cdot 6NH_3\ (s.)$, $CoCl_2\ (s.) \rightarrow CoCl_2 \cdot 2H_2O\ (s.) \rightarrow CoCl_2 \cdot 6H_2O\ (s.)$, $CoNO_3\ (s.) \rightarrow CoNO_3 \cdot 2H_2O\ (s.) \rightarrow CoNO_3 \cdot 4H_2O\ (s.) \rightarrow CoNO_3 \cdot 6H_2O\ (s.)$ and from the change in the increment to ΔH_f° upon the $H_2O \rightarrow NH_3$ ligand replacement with the heats of formation $\Delta H_f^\circ[NH_3] = -46.0$ (gas), -67.2 (l.) kJ mol^{-1},[9] $\Delta H_f^\circ[H_2O] = -241.6$ (gas), -285.9 (l.) kJ mol^{-1} [9] with the assumption that the replacement of the H_2O ligand by $CH_2CHCONH_2$ results in a decrease in ΔH_f° by ~33.0 kJ mol^{-1}. The $\Delta H_f^\circ[CH_2{=}CHCONH_2\ (gas)]$ value was calculated with the assumption that $\Delta H_f^\circ[CH_2CHCOOH\ (gas)] = -426.4$ kJ mol^{-1} [8] and that the replacement of the —C(O)OH fragment by —C(O)NH$_2$ results in the gain in ΔH_f° equal to 159 kJ mol^{-1}.[10]

The water and acrylamide vapors formed during the thermolysis can be removed from the reaction area, being condensed on cold walls of the reaction vessel (~20 °C); this was observed experimentally.

An increase in T_{therm} (> 360 K) induces polymerization of the dehydrated complex.

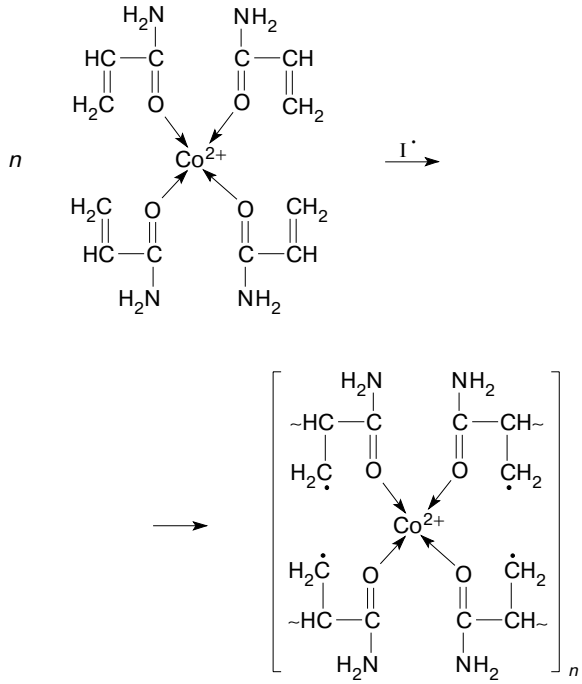

Polymerization of this monomer is accompanied by evolution of a fairly large amount of heat; more precisely, the heat of polymerization per mole of double bonds, apparently, does not differ significantly from the heat of polymerization of free acrylamide, which is equal to ~83 kJ mol^{-1} for solution polymerization;[11] however, it cannot be ruled out that complexation decreases the heat of polymerization.

Nitrogen oxides (N_2O, NO), detected experimentally during the solid-phase thermolysis of **1**, appear to arise both upon the thermal decomposition of HNO_3 [12] and its reaction with NH_3 or directly with the AAm amino group and upon the possible transformation of the mononuclear complex **1** into a binuclear cluster, similar to dimeric μ-oxo complexes.[13—15] The appearance of NH_3 and HNO_3 can be due to the reaction of the H_2O vapor formed upon dehydration with the AAm ligand and the NO_3^- anion of **1** in the reaction area.

Nitrogen oxides (N_2O_5, NO_3, NO, NO_2)[12] are fairly reactive and can undergo subsequent transformations. On the one hand, these species can initiate radical polymerization of the dehydrated monomer[4] (NO and NO_2 are known[16,17] to initiate polymerization of AAm in solutions). On the other hand, these species can be consumed in the extensive oxidation of organic ligands giving CO and CO_2 and accompanied by substantial heat evolution. However, in the temperature range studied, the yields of CO, CO_2, and N_2O at the end of gas

evolution (in the self-generated atmosphere) is lower than that expected upon complete oxidation of the initial product. The particular mechanism of the thermooxidative destruction of the resulting polymer is not entirely clear now and requires further investigations.

Attention is attracted by the following fact. At the end of gas evolution, solid-phase products are diamagnetic, *i.e.*, the thermolyzed material contains no Co-containing para- and/or ferromagnetic phases (Co, CoO, Co_2O_3).[18] The magnetic properties of the resulting product show themselves only in the case of thermolysis of acrylamide complex **1** in air at $T_{therm} > 680$ K. It can be suggested that the solid-phase products formed at the end of transformations in a self-generated atmosphere have resulted from the interaction of the Co atoms with the polymer matrix, as indicated by the data of electron microscopy (see Fig. 4). In other words, at relatively low temperatures of thermolysis, very small particles stabilized by the polymer matrix are formed, whereas at higher temperatures, they become larger and the resulting domains exhibit magnetic properties. A similar phenomenon has been observed previously in a study of the pyrolysis of cobalt carbonyls in a polybutadiene matrix.[19]

Thus, thermolysis of complex **1** is a multistage process, which includes the following three macro stages: dehydration, polymerization of the dehydrated monomer, and thermooxidative destruction of the resulting polymer. The exothermicity of the last two stages can be one of the main reasons for the development of the frontal polymerization process. Substantial heat evolution in the oxidative destruction of the polymer at the third stage of transformations under definite heat and mass transfer conditions can bring about an "extremal" pattern of gas evolution.

The authors are grateful to N. V. Chukanov for the assistance in the interpretation of the IR absorption spectra of the products of transformation of complex **1** and to S. I. Evstratova for providing the initial sample of **1**.

This study was supported by the Russian Foundation for Basic Research (Project No. 01-03-33257).

References

1. V. A. Ershova, A. V. Golovin, L. A. Sheludyakova, P. P. Semyannikov, S. I. Pomogailo, and A. D. Pomogailo, *Izv. Akad. Nauk, Ser. Khim.*, 2000, 1455 [*Russ. Chem. Bull., Int. Ed.*, 2000, **49**, 1448].
2. V. S. Savost´yanov, V. I. Ponomarev, A. D. Pomogailo, B. S. Selenova, I. N. Ivleva, A. G. Starikov, and L. O. Atovmyan, *Izv. Akad. Nauk SSSR. Ser. Khim.*, 1990, 762 [*Bull. Acad. Sci. USSR, Div. Chem. Sci.*, 1990, **39**, 674 (Engl. Transl.)].
3. V. S. Savost´yanov, A. D. Pomogailo, B. S. Selenova, D. A. Kritskaya, and A. N. Ponomarev, *Izv. Akad. Nauk SSSR, Ser. Khim.*, 1990, 768 [*Bull. Acad. Sci. USSR, Div. Chem. Sci.*, 1990, **39**, 680 (Engl. Transl.)].
4. V. S. Savost´yanov, G. P. Belov, D. A. Kritskaya, A. D. Pomogailo, and A. N. Ponomarev, *Izv. Akad. Nauk SSSR, Ser. Khim.,* 1990, 1015 [*Bull. Acad. Sci. USSR, Div. Chem. Sci.*, 1990, **39**, 905 (Engl. Transl.)].
5. *Entsiklopediya polimerov*, Sov. entsiklopediya, Moscow, 1972, **1**, 30 (in Russian).
6. S. P. Davtyan, V. P. Zhirkov, and S. A. Vol´fson, *Usp. Khim.*, 1984, **53**, 251 [*Russ. Chem. Rev.*, 1984, **53** (Engl. Transl.)].
7. *Khimicheskaya entsiklopediya,* Sov. entsiklopediya, Moscow, 1988, **1**, 116 (in Russian).
8. K. V. Yatsimirskii, *Termokhimiya kompleksnykh soedinenii* [*Thermochemistry of Complexes*], Izd-vo Akad. Nauk SSSR, Moscow, 1951, 251 pp. (in Russian).
9. M. Kh. Karapet´yants and M. L. Karapet´yants, *Osnovnye termodinamicheskie konstanty neorganicheskikh i organicheskikh veshchestv* [*Main Thermodynamic Constants of Inorganic and Organic Compounds*], Khimiya, Moscow, 1968, 470 pp. (in Russian).
10. L. V. Gurvich, G. V. Karachevtsev, V. N. Kondrat´ev, Yu. A. Lebedev, V. A. Medvedev, V. K. Potapov, and Yu. S. Khodeev, *Energii razryva khimicheskikh svyazei. Potentsialy ionizatsii i srodstvo k elektronu* [*Energies of Chemical Bond Cleavage. Ionization Potentials and Electron Affinities*], Nauka, Moscow, 1974, 351 pp. (in Russian).
11. C. T. Mortimer, *Reactions Heats and Bond Strength*, Pergamon Press, Oxford—London—New York—Paris, 1962.
12. Yu. I. Rubtsov and A. I. Kazakov, in *Gorenie i vzryv, Mater. chetvertogo vsesoyuz. simpoz. po goreniyu i vzryvu* [*Combustion and Explosion. Fourth All-Union Symposium on Combustion and Explosion*], *Proc., Chernogolovka, September 23—27, 1974*, Nauka, Moscow, 1977, 600 (in Russian)..
13. M. A. Porai-Koshits, in *Kristallokhimiya* [*Crystal Chemistry*], *Itogi nauki i tekhniki,* VINITI Akad. Nauk SSSR, Moscow, 1981, **15**, 13 (in Russian).
14. A. D. Negro, L. Ungaretti, and A. Perrotti, *J. Chem. Soc., Dalton Trans.,* 1972, **15**, 1639.
15. D. P. Bullivant, M. F. A. Dove, and M. J. Haley, *J. Chem. Soc., Chem. Commun.,* 1977, 584.
16. (a) M. K. Mishra, *Macromol. Chem., Rapid Commun.,* 1985, **6**, 541; (b) M. K. Mishra, *J. Appl. Polym. Sci.,* 1985, **30**, 725.
17. S. N. Bhadant and T. K. Prasad, *Macromol. Chem.,* 1980, **191**, 1085.
18. D. D. Mishin, *Magnitnye materialy*, Vyssh. shkola, Moscow, 1991, 384 s.
19. L. M. Bronstein, S. P. Solodovnikov, E. Sh. Mirzoeva, E. Yu. Baukova, and P. M. Valetsky, *Proc. Am. Chem. Soc., Div. Polym. Mater. Sci. Engin.,* 1994, **71**, 397.

Received January 3, 2000;
in revised form May 15, 2000